Hydrology and
Earth System
Sciences

Does the Budyko curve reflect a maximum-power state of hydrological systems? A backward analysis

M. Westhoff[1], E. Zehe[2], P. Archambeau[1], and B. Dewals[1]

[1]Department of Hydraulics in Environmental and Civil Engineering (HECE), University of Liege (ULg), Liege, Belgium
[2]Karlsruhe Institute of Technology (KIT), Karlsruhe, Germany

Correspondence to: M. Westhoff (martijn.westhoff@ulg.ac.be)

Abstract. Almost all catchments plot within a small envelope around the Budyko curve. This apparent behaviour suggests that organizing principles may play a role in the evolution of catchments. In this paper we applied the thermodynamic principle of maximum power as the organizing principle.

In a top-down approach we derived mathematical formulations of the relation between relative wetness and gradients driving run-off and evaporation for a simple one-box model. We did this in an inverse manner such that, when the conductances are optimized with the maximum-power principle, the steady-state behaviour of the model leads exactly to a point on the asymptotes of the Budyko curve. Subsequently, we added dynamics in forcing and actual evaporation, causing the Budyko curve to deviate from the asymptotes. Despite the simplicity of the model, catchment observations compare reasonably well with the Budyko curves subject to observed dynamics in rainfall and actual evaporation. Thus by constraining the model that has been optimized with the maximum-power principle with the asymptotes of the Budyko curve, we were able to derive more realistic values of the aridity and evaporation index without any parameter calibration.

Future work should focus on better representing the boundary conditions of real catchments and eventually adding more complexity to the model.

1 Introduction

In different climates, partitioning of rainwater into evaporation and run-off is different as well. Yet, when plotting the evaporation fraction against the aridity index (ratio of potential evaporation to rainfall), almost all catchments plot in a small envelope around a single empirical curve known as the Budyko curve (Budyko, 1974). The fact that almost all catchments worldwide plot within this small envelope around this curve inspired several scientists to speculate whether this is due to co-evolution of climate and terrestrial catchment characteristics (e.g. Harman and Troch, 2014). Co-evolution between climate and the terrestrial system could in turn be explained by an underlying organizing principle which determines optimum system functioning (Sivapalan et al., 2003; McDonnell et al., 2007; Schaefli et al., 2011; Thompson et al., 2011; Ehret et al., 2014; Zehe et al., 2014). As hydrological processes are essentially dissipative, we suggest that thermodynamic-optimality principles are deemed to be very interesting candidates.

The most popular among these are the closely related principles of maximum entropy production (Kleidon and Schymanski, 2008; Kleidon, 2009; Porada et al., 2011; Wang and Bras, 2011; del Jesus et al., 2012; Westhoff and Zehe, 2013) and maximum power (Kleidon and Renner, 2013; Kleidon et al., 2013; Westhoff et al., 2014) on the one hand – both defining the optimum configuration between competing fluxes across the system boundary – and, on the other hand, minimum energy dissipation (Rinaldo et al., 1992; Rodriguez-Iturbe et al., 1992; Hergarten et al., 2014) or maximum free-energy dissipation (Zehe et al., 2010, 2013), focusing on free-energy dissipation associated with changes

in internal state variables as a result of boundary fluxes, i.e. soil moisture and capillary potential, and a related optimum system configuration. In this research we focus on the maximum-power principle.

The validity and the practical value of thermodynamic-optimality principles are still debated (e.g. Dewar, 2009), and the partly promising results reported in the above-listed studies might be just a matter of coincidence. There is a vital search for defining rigorous tests to assess how far thermodynamic-optimality principles apply. The Budyko curve appears very well suited for such a test, as it condenses relative weights of the steady-state water fluxes in most catchments around the world. It is thus not astonishing that there have been several attempts to reconcile the Budyko curve with thermodynamic-optimality principles. For example, Porada et al. (2011) used the maximum-entropy-production principle to optimize the run-off conductance and evaporation conductance of a bucket model being forced with observed rainfall and potential evaporation of the 35 largest catchments in the world. The resulting modelled fluxes were plotted in the Budyko diagram and followed the curve with a similar scatter as real-world catchments.

Another very interesting approach was presented by Kleidon and Renner (2013) and Kleidon et al. (2014), using the perspective of the atmosphere. They maximized power of the vertical convective motion transporting heat and moisture upwards using the Carnot limit to constrain the sensible heat flux. This motion is driven by the temperature differences between the surface and the atmosphere, while at the same time depleting this temperature gradient, leading to a maximum in power. Additionally, evaporation at the surface and condensation in the atmosphere deplete this gradient even further at the expense of more vertical moisture transport and thus more convective motion. Their approach showed some more spreading around the Budyko curve for the same 35 catchments as used in Porada et al. (2011), but they used a simpler model that has to be forced with far fewer observations, namely solar radiation, precipitation, and surface temperature.

Very recently, Wang et al. (2015) used the maximum-entropy-production principle to derive directly an expression for the Budyko curve. They started from the expression of Kleidon and Schymanski (2008), and by maximizing the entropy production of the whole system they reached the expression for the Budyko curve as formulated by Wang and Tang (2014). This is an intriguing result that partly contradicts the findings of Westhoff and Zehe (2013), whose study revealed, in simulations with an HBV type conceptual model, that joint optimization of overall entropy production results in optimum conductances approaching zero.

The objective of this study is to define a model which, under constant forcing, leads to a point on the asymptotes of the Budyko curve when flow conductances are optimized by maximizing power. The model is comparable to the one proposed by Porada et al. (2011), but with different relations

between relative wetness of the subsurface store and driving gradients. We derived the gradients driving evaporation and run-off in an inverse manner, with both the asymptotes of the Budyko curve and the maximum-power principle as constraints. Subsequently, we added dynamics in forcing or in actual evaporation (similar to Westhoff et al., 2014) to move away from these asymptotes to more realistic values of the aridity and evaporation index, without calibrating any parameter. Finally, these sensitivities were compared to observations.

2 The maximum-power principle

The maximum-power principle implies that a system evolves in such a way that steady-state fluxes across a systems boundary produce maximum power. It is directly derived from the first and the second laws of thermodynamics, and it is very well explained in Kleidon and Renner (e.g. 2013). Here we give only a short description: let us start by considering a warm and a cold reservoir, which are connected to each other. The warm reservoir is forced by a constant energy input J_{in}, and the cold reservoir is cooled by a heat flux J_{out}. In steady state $J_{in} = J_{out}$ and both reservoirs have a constant temperature T_h and T_c, respectively, with $T_h > T_c$. The heat flux between the two reservoirs produces entropy, which is given by

$$\sigma = \frac{J_{out}}{T_c} - \frac{J_{in}}{T_h}. \tag{1}$$

However, instead of transferring all incoming energy to the cold reservoir, the heat gradient can also be used to perform work (to create other forms of free energy). This means that, in steady state, the incoming energy flux J_{in} equals the outgoing energy flux J_{out} plus the rate of work P (which is power) performed by the system.

For given temperatures of both reservoirs, the theoretical maximum rate of work is given by the Carnot limit:

$$P_{Carnot} = J_{in} \frac{T_h - T_c}{T_h}. \tag{2}$$

Now we introduce an extra flux cooling the hot reservoir as a function of its temperature $J_{h.out} = f(T_h)$. This flux is in competition with the flux $J_{h\text{-}c}$ between both reservoirs, while both reduce the temperature gradient between the two reservoirs. In Eq. (2) J_{in} should then be replaced by $J_{h\text{-}c}$, while T_h and T_c are not fixed anymore but are a function of all fluxes. In this setting, there exists a flux $J_{h\text{-}c}$ maximizing power. In the extreme cases of $J_{h\text{-}c} = 0$ and $J_{h\text{-}c} \to \infty$, power is zero, while for intermediate values power is larger than zero.

In hydrological systems, power is often generated by water fluxes and is given as the product of a mass flux and the potential difference driving this flux, (note that several authors have divided this formulation by the absolute temperature, while naming it maximum entropy production: e.g.

Kleidon and Schymanski, 2008; Porada et al., 2011; Westhoff and Zehe, 2013; Westhoff et al., 2014; Kollet, 2015). Although these formulations are equivalent in isothermal circumstances, the here-derived maximum-power principle is, in our opinion, more sound.

In the remainder of this article we use specific water fluxes $(L\,T^{-1})$ and potential differences $\mu_{high} - \mu_{low}$ in meter water column (L), where the flux is given as the product of a specific conductance k (T^{-1}) and the potential difference. We recognize that, in order to come to the same units as power, these formulations should be multiplied by the water density, gravitational acceleration, and a cross-sectional area, but since we are looking for a maximum, and these parameters are constant, we can leave them out. We also use the word gradient for the potential difference $\mu_{high} - \mu_{low}$, where the length scale with which the difference should be divided is incorporated into the conductance. With these formulation, power is given by

$$P = k\left(\mu_{high} - \mu_{low}\right)^2, \tag{3}$$

where k is the free parameter we optimized to find a maximum in power.

3 Mathematical framework

Here we derive the model that, when conductances are optimized with the maximum-power principle, always results in a point on the asymptotes of the Budyko curve independent of the value of the given constant atmospheric inputs (here rainfall and chemical potential of the atmosphere). To reach this, proper relations between relative wetness and gradients driving run-off and evaporation were derived, which is explained in the following.

3.1 Initial model setup

Our model consists of a simple reservoir being filled by rainfall Q_{in} and drained by evaporation E_a and run-off Q_r. Using the same expressions as in Kleidon and Schymanski (2008), the steady-state mass balance and corresponding fluxes are expressed by

$$Q_{in} = E_a + Q_r, \tag{4}$$
$$E_a = k_e\left(\mu_s - \mu_{atm}\right), \tag{5}$$
$$Q_r = k_r\left(\mu_s - \mu_r\right), \tag{6}$$

where μ_s, μ_r, and μ_{atm} are the chemical potential of the soil, chemical potential of the free water surface of the nearest river, and chemical potential of the atmosphere, respectively, while k_e and k_r are the specific conductances of evaporation and run-off. In these expressions, μ_s and $\mu_s - \mu_r$ are func-

tions of the relative saturation h in the reservoir:

$$G_e(h) = \mu_s(h), \tag{7}$$
$$G_r(h) = \mu_s(h) - \mu_r(h), \tag{8}$$

where $G_e(h)$ and $G_r(h)$ can have any form as long as they are strictly monotonically increasing with increasing relative saturation. For example, Porada et al. (2011) used the van Genuchten model (van Genuchten, 1980) and gravitational potential to derive the chemical potential of the soil. However, here we will derive them in such a way that, under constant forcing, we end up exactly at the Budyko curve.

3.2 Backward analysis to determine the driving gradients

3.2.1 Optimum k_e^* matching the Budyko curve

Let us first find an optimum conductance k_e^* leading to a point on the asymptotes of the Budyko curve B. An expression describing these asymptotes exactly is given by (adapted from Wang and Tang, 2014)

$$B = \frac{E_a}{Q_{in}} = \frac{1 + E_{pot}/Q_{in} - \sqrt{\left(E_{pot}/Q_{in} - 1\right)^2}}{2}, \tag{9}$$

with E_{pot} being the potential evaporation. Now we make an important assumption to define E_{pot}: we assume that evaporation is purely described as the product of a gradient and conductance – ignoring the influence of radiation. It is assumed to be maximum when in Eqs. (5) and (8) $\mu_s = 0$, meaning that the relative wetness is 1, implying no water limitation. With this assumption, potential evaporation is given by $E_{pot} = k_e^*(-\mu_{atm})$ (note that μ_{atm} is always negative). Combining this equation with Eqs. (5), (7), and (9) results in

$$k_e^* = \frac{Q_{in}}{\left(G_e(h^*) - \mu_{atm}\right)} B(k_e^*), \tag{10}$$

where h^* is the steady-state relative wetness leading to a point on the asymptotes of the Budyko curve (note that this is the relative wetness occurring when $k_e = k_e^*$).

3.2.2 Maximum power by evaporation

As mentioned above, k_e^* should also correspond to a maximum in power by evaporation (P_e). We achieved this in a backward analysis, implying that we start with defining a function $P_e(k_e)$ which is always larger than zero for $k_e \in (0, +\infty)$ and where $\partial P_e/\partial k_e = 0$ at $k_e = k_e^*$. A function sat-

isfying these constraints is[1]

$$P_{\rm e}(k_{\rm e}) = k_{\rm e} \frac{P_0}{k_0} e^{-\left(\frac{k_{\rm e}-a}{k_0}\right)^2}, \tag{11}$$

where P_0 and k_0 are the reference power ($\mathrm{L^2 T^{-1}}$) and reference conductance ($\mathrm{T^{-1}}$), introduced to come to the correct units. In all computations they have been set to unity. Setting the derivative to zero for $k_{\rm e} = k_{\rm e}^*$ yields

$$\frac{\partial P_{\rm e}}{\partial k_{\rm e}} = \left(2k_{\rm e}^* a - 2k_{\rm e}^{*2} + k_0^2\right) \frac{P_0}{k_0^3} e^{-\left(\frac{k_{\rm e}^*-a}{k_0}\right)^2} = 0 \tag{12}$$

$$\rightarrow a = k_{\rm e}^* - \frac{k_0^2}{2k_{\rm e}^*},$$

resulting in $P_{\rm e}(k_{\rm e}) = k_{\rm e} P_0 / k_0 e^{-((k_{\rm e}-k_{\rm e}^*)/k_0 + k_0/(2k_{\rm e}^*))^2}$.

Combining this expression with Eqs. (3) and (7) ($P_{\rm e} = k_{\rm e}(G_{\rm e} - \mu_{\rm atm})^2$), $G_{\rm e}$ is expressed as

$$G_{\rm e}(k_{\rm e}) = \pm\sqrt{\frac{P_0}{k_0} e^{-\left(\frac{k_{\rm e}-k_{\rm e}^*}{k_0} + \frac{k_0}{2k_{\rm e}^*}\right)^2}} + \mu_{\rm atm}. \tag{13}$$

Since we neglect condensation ($G_{\rm e}(k_{\rm e}) - \mu_{\rm atm} \geq 0$), only the positive solution remains. Inserting Eq. (13) into Eq. (10) and setting $k_{\rm e} = k_{\rm e}^*$ yields

$$k_{\rm e}^* = \frac{Q_{\rm in}}{\sqrt{\frac{P_0}{k_0} e^{-\frac{k_0^2}{4k_{\rm e}^{*2}}}}} B(k_{\rm e}^*), \tag{14}$$

which can be solved iteratively for $k_{\rm e}^*$.

Combining these results with the mass balance (Eqs. 4–6) yields the following expression for run-off gradient $G_{\rm r}$ as a function of $k_{\rm e}$:

$$G_{\rm r}(k_{\rm e}) = \frac{Q_{\rm in}}{k_{\rm r}} - \frac{k_{\rm e}}{k_{\rm r}} \sqrt{\frac{P_0}{k_0} e^{-\left(\frac{k_{\rm e}-k_{\rm e}^*}{k_0} + \frac{k_0}{2k_{\rm e}^*}\right)^2}}. \tag{15}$$

Note that any value of $k_{\rm r}$ leads to a point on the Budyko curve.

3.2.3 Maximum power by run-off

Although the Budyko curve does not depend on the value of $k_{\rm r}$, an optimum $k_{\rm r}^*$ can still be found by maximizing power by run-off. For this, steps similar to those for optimizing $k_{\rm e}$ are used, where in Eqs. (11)–(13) $k_{\rm e}$ is simply replaced by $k_{\rm r}$, resulting in a gradient for run-off as a function of $k_{\rm r}$:

$$G_{\rm r}(k_{\rm r}) = \sqrt{\frac{P_0}{k_0} e^{-\left(\frac{k_{\rm r}-k_{\rm r}^*}{k_0} + \frac{k_0}{2k_{\rm r}^*}\right)^2}}, \tag{16}$$

---

[1]We have also tested the function $P_{\rm e}(k_{\rm e}) = P_0 exp\left(-((k_{\rm e}-a)/k_0)^2\right)$, but this led to two non-trivial solutions for $k_{\rm e}^*$ and is thus less convenient to use than the expression in Eq. (11)

while from the mass balance (Eqs. 4–8), $k_{\rm r}$ is given by

$$k_{\rm r} = \frac{Q_{\rm in} - [G_{\rm e}(h) - \mu_{\rm atm}]}{G_{\rm r}(h)}. \tag{17}$$

Combining these two equations and setting $k_{\rm r}$ to $k_{\rm r}^*$ yields

$$k_{\rm r}^* = \frac{Q_{\rm in} - k_{\rm e}^*\left[G_{\rm e}(k_{\rm e}^*) - \mu_{\rm atm}\right]}{\sqrt{\frac{P_0}{k_0} e^{-\frac{k_0^2}{4k_{\rm r}^{*2}}}}}, \tag{18}$$

which can also be solved iteratively for $k_{\rm r}^*$.

3.3 Forward analysis

To apply the maximum-power principle in any hydrological model, the model should run until a (quasi-)steady state is reached. Within the above-presented backward analysis the steady-state optimum gradients are simply found by giving $k_{\rm e}$ the value of $k_{\rm e}^*$ in Eq. (13) and $k_{\rm r} = k_{\rm r}^*$ in Eq. (15).

However, when the relative wetness h evolves over time, the gradients should be resolved as a function of the relative wetness ($G_{\rm e} = G_{\rm e}(h)$ and $G_{\rm r} = G_{\rm r}(h)$). To do this, we assumed that h is a linear function of $G_{\rm r}(k_{\rm e})$ scaled between zero and unity (for sensitivities to different initial relations between relative wetness and one of the gradients see Supplement S1):

$$G_{\rm r}(h) = \min[G_{\rm r}(k_{\rm e})] + (\max[G_{\rm r}(k_{\rm e})] - \min[G_{\rm r}(k_{\rm e})]) h, \tag{19}$$

where the maximum in $G_{\rm r}(k_{\rm e})$ occurs when the second term on the right-hand side of Eq. (15) is zero ($\max[G_{\rm r}(k_{\rm e})] = \frac{Q_{\rm in}}{k_{\rm r}}$) and the minimum value is derived when this second term is maximum, occurring at $k_{\rm e} = k_{\rm e}^{\max} = 1/2\left(k_{\rm e}^* - \frac{k_0^2}{2k_{\rm e}^*} + \sqrt{\left(k_{\rm e}^* - \frac{k_0^2}{2k_{\rm e}^*}\right)^2 + 4}\right)$. Inserting this into Eq. (15) yields

$$\min[G_{\rm r}(k_{\rm e})] = \frac{Q_{\rm in}}{k_{\rm r}} - \frac{k_{\rm e}^{\max}}{k_{\rm r}} \sqrt{\frac{P_0}{k_0} e^{-\left(\frac{k_{\rm e}^{\max}-k_{\rm e}^*}{k_0} + \frac{k_0}{2k_{\rm e}^*}\right)^2}}. \tag{20}$$

If we now plot h vs. $G_{\rm e}$, a unique relation between the two exists (Fig. 1).

With the gradients as functions of h, the non-steady mass balance equation is written as

$$S_{\max} \frac{\mathrm{d}h}{\mathrm{d}t} = Q_{\rm in} - k_{\rm r} G_{\rm r}(h) - k_{\rm e}\left(G_{\rm e}(h) - \mu_{\rm atm}\right), \tag{21}$$

where $S_{\max}$ is the maximum storage depth (L) and t is time (T). Now, the time evolution of the relative wetness can be simulated.

4 Results and discussion from forward analysis

4.1 Constant forcing

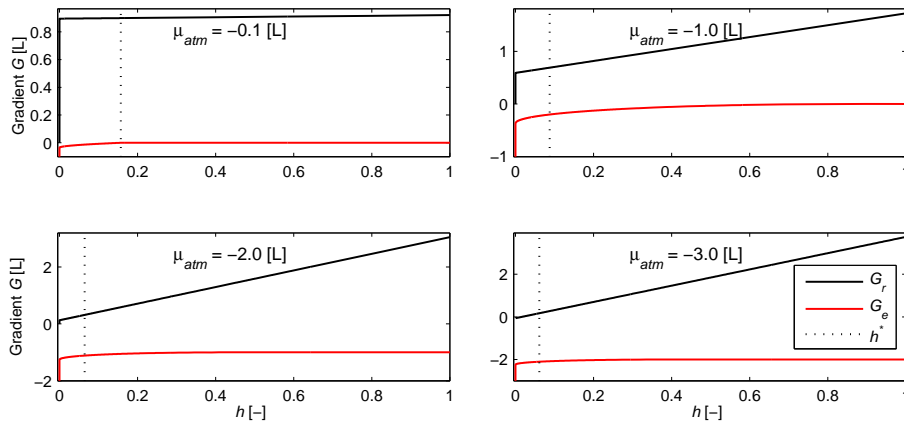With the known relations between relative wetness and gradients driving evaporation and run-off, the forward model was

Figure 1. The gradients driving evaporation (G_e) and run-off (G_r) as a function of the relative saturation (h) for different values of μ_{atm} with $k_r = k_r^*$. At $h = 0$, the slope of the gradient G_e is vertical, while the value of G_r is set to zero to avoid run-off at zero saturation.
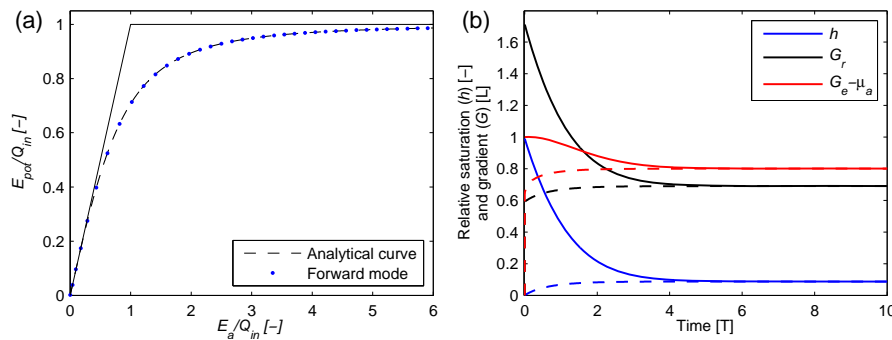

Figure 2. (a) Analytical Budyko curve (Eq. 9) and result from forward mode with constant forcing and **(b)** time evolution of relative saturation and both gradients for complete initial saturation (solid lines) and initial dry state (dashed lines). $\mu_{atm} = -0.7$.

run and k_e was optimized by maximizing power. With constant forcing, each value of μ_{atm} resulted in a point on the asymptotes of the Budyko curve (Fig. 2a). In Fig. 2b, the time evolution of the relative wetness and both gradients are shown for an initially saturated and an initially dry state, indicating that, irrespective of the initial state, the forward model evolves to a steady state.

4.2 Sensitivity to dry spells

By introducing dynamics in forcing, we expected the resulting Budyko curve to deviate from the asymptotes.

In the literature, the deviation from the asymptotes is often done by introducing an empirical parameter (e.g. Choudhury, 1999; Wang and Tang, 2014).

To move away from this empiricism, we started at the asymptotes of the Budyko curve. Subsequently, we added dry spells and dynamics in evaporation (e.g. when trees lose their leaves the evaporative conductance k_e goes to zero) and tested how this influenced the Budyko curve.

To test sensitivities to dry spells, simple block functions were used, with either a predefined constant input or no in-

put at all. For longer relative lengths of the dry spell, the slope of the curves becomes smaller until a maximum of $E_a/Q_{in} = 0.98$ (Fig. 3). The reason the asymptotes do not reach unity lies in the fact that already at very short dry spells a second maximum in power evolves, while the first maximum disappears quickly with increasing dry spells. This is in line with results of Westhoff et al. (2014), and in Zehe et al. (2013) a second optimum is also present. Although interesting, we leave a better exploration of this transition zone where two maxima exist for future research.

These curves were compared with data of real catchments that have a relatively stable wet period interspersed with a regular dry period. The Mupfure catchment (Zimbabwe, Savenije, 2004), with approximately 7 months without rain (Fig. S2.1 of Supplement), plots very close to the theoretical curve with the same length of the dry spell. However, catchments from the Model Parameter Estimation Experiment (MOPEX) database (Schaake et al., 2006) with clear, consistent dry spells still plot far from the respective theoretical curves. This discrepancy can be partly explained by the somewhat arbitrary way the number of dry months is determined: the MOPEX catchments are filtered to have only
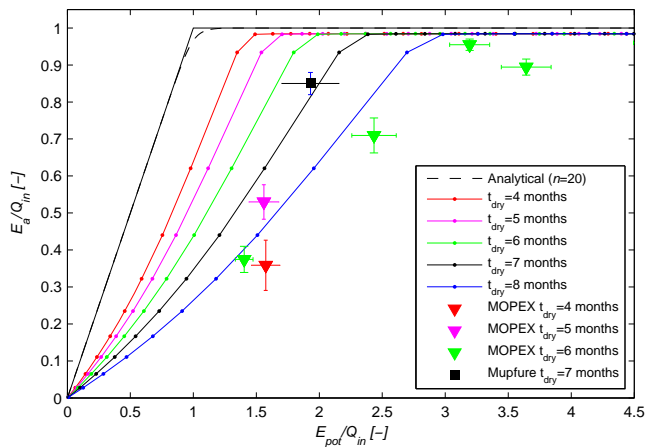
Figure 3. Sensitivity to periodic dry spells in the forward model. MOPEX catchments are filtered to have only those catchments having at least 1 month with a median rainfall $< 2.5 \, \mathrm{mm \, month^{-1}}$ and a coefficient of variance < 0.5 for all months with a median rainfall $> 25 \, \mathrm{mm \, month^{-1}}$. The final number of dry months was determined maximizing the difference between the mean monthly precipitation of the X driest months minus the mean monthly precipitation of the $1 - X$ wettest months, where $X = 1, 2 \ldots 12$. Error bars indicate 1 standard deviation and are determined with bootstrap sampling.

those catchments having at least 1 month with a median rainfall $< 2.5 \, \mathrm{mm \, month^{-1}}$ and a coefficient of variance < 0.5 for all months with a median rainfall $> 25 \, \mathrm{mm \, month^{-1}}$. The final number of dry months was determined maximizing the difference between the mean monthly precipitation of the X driest months minus the mean monthly precipitation of the $1 - X$ wettest months, where $X = 1, 2 \ldots 12$.

For example, the MOPEX catchment with a 4-month dry spell could also be argued to have a dry spell of 7 months (Fig. S2.1, MOPEX ID: 11222000); similarly, the MOPEX catchment with a 5-month dry spell (Fig. S2.1, MOPEX ID: 11210500) could also be argued to have one of 6 months. If these "corrections" are made, the variability within the MOPEX catchments is consistent (with longer dry spells plotting more to the right), but there is still a discrepancy with the simulated curves of 1 to 2 months, indicating that the model should still be improved.

4.3 Sensitivity to dynamics in actual evaporation

We also tested the sensitivity of dynamics in actual evaporation by periodically turning k_e on and off, while keeping the rainfall constant. This sensitivity analysis shows that the longer actual evaporation is switched off, the smaller the slope of the Budyko curve and the smaller the maximum value of the evaporation index (Fig. 4). Comparing the different curves with real catchments shows that data from the Ourthe catchment (Belgium) are relatively close to its respective line (its months without actual evaporation are estimated
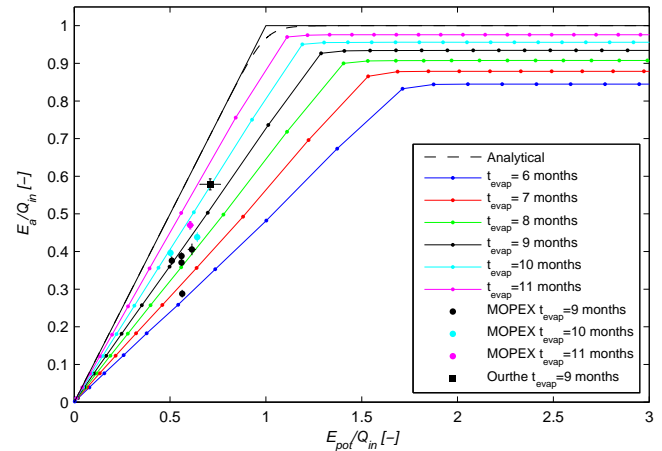

Figure 4. Sensitivity to on–off dynamics in actual evaporation in the forward model. MOPEX catchments were filtered to have only those catchments having a coefficient of variance < 0.12 for monthly median rainfall and with at least 1 month with a median maximum air temperature $< 0\,^{\circ}\mathrm{C}$; a month is considered to have no actual evaporation if the monthly median maximum air temperature $< 0\,^{\circ}\mathrm{C}$ (after Devlin, 1975). Error bars indicate 1 standard deviation and are determined with bootstrap sampling.

from Fig. 6.1 of Aalbers, 2015). Also the MOPEX catchments plot relatively close to their respective lines. However, the way the MOPEX catchments were filtered is somewhat arbitrary (only those having a coefficient of variance < 0.12 for monthly median rainfall and with at least 1 month with a monthly median maximum ambient temperature $< 0\,^{\circ}\mathrm{C}$ are taken into account; a month is considered to have no actual evaporation if the monthly median maximum air temperature $< 0\,^{\circ}\mathrm{C}$; after Devlin, 1975, Fig. S2.2 of Supplement).

At first sight the comparison with data looks better than in the case of dry spells. However, all plotted catchments have an aridity index between 0.5 and 0.71, and within this range the different curves also plot close to each other. Yet, it is still somewhat surprising that the comparison is relatively good, since the modelled lines were created by assuming a constant atmospheric demand (μ_{atm}) for each run, which is different from real catchments that have a more-or-less sinusoidal potential evaporation over the year. However, we consider it as future work to better represent the real-world dynamics in the model.

5 Conclusions and outlook

The Budyko curve is empirical proof that only a subset of all possible combinations of aridity index and evaporation index emerges in nature. It belongs to the so-called Darwinian models (Harman and Troch, 2014), focusing on emergent behaviour of a system as a whole. Since the maximum-power principle links Newtonian models with the Darwinian mod-

els, it has indeed potential to derive the Budyko curve with an, in essence, Newtonian model.

We presented a top-down approach in which we derived relations between relative wetness and chemical potentials that lead, under constant forcing, to a point on the asymptotes of the Budyko curve when the maximum-power principle is applied. Subsequently sensitivities to dynamics in forcing and actual evaporation were tested.

Since the Budyko curve is an empirical curve, a calibration parameter is often linked to catchment-specific characteristics such as land use, soil water storage, climate seasonality, or spatial scales (e.g. Milly, 1994; Yang et al., 2008; Choudhury, 1999; Zhang et al., 2004; Potter et al., 2005). Although correlations between characteristics and the calibration parameter have been found, it remains a calibration parameter.

Here we presented a method to derive the Budyko curve without any calibration parameter, but sensitive to temporal dynamics in boundary conditions. Although we used simple block functions to test these sensitivities, they compare reasonably well with observations. Nevertheless, improvements could be made by modelling dynamics closer to reality, or even by adding multiple parallel reservoirs to account for spatial variability within a catchment.

Even though the model represents observations reasonably well (despite its simplicity), the method used here is by no means proof that the maximum-power principle applies for hydrological systems. This is due to the top-down derivation of the gradients in which the maximum-power principle is used explicitly. In principle, the method could also be used with respect to any other optimization principle. However, the reasonable fits with observations are grounds upon which to further explore this methodology – including the maximum-power principle.

The Supplement related to this article is available online at doi:10.5194/hess-20-479-2016-supplement.

References

Aalbers, E.: Evaporation in conceptual rainfall-runoff models: testing model realism using remotely sensed evaporation, Master's thesis, Delft University of Technology, available at: http://repository.tudelft.nl/view/ir/uuid:a2edc688-2270-4823-aa93-cb861cf481a2/, last access: 10 August 2015.

Budyko, M. I.: Climate and Life, 508 pp., Academic Press, New York , 1974.

Choudhury, B.: Evaluation of an empirical equation for annual evaporation using field observations and results from a biophysical model, J. Hydrol., 216, 99–110, doi:10.1016/S0022-1694(98)00293-5, 1999.

del Jesus, M., Foti, R., Rinaldo, A., and Rodriguez-Iturbe, I.: Maximum entropy production, carbon assimilation, and the spatial organization of vegetation in river basins, P. Natl. Acad. Sci. USA, 109, 20837–20841, doi:10.1073/pnas.1218636109, 2012.

Devlin, R.: Plant Physiology, 3rd Edn., D. Van Nostrand Company, New York, 1975.

Dewar, R. C.: Maximum Entropy Production as an Inference Algorithm that Translates Physical Assumptions into Macroscopic Predictions: Don't Shoot the Messenger, Entropy, 11, 931–944, doi:10.3390/e11040931, 2009.

Ehret, U., Gupta, H. V., Sivapalan, M., Weijs, S. V., Schymanski, S. J., Blöschl, G., Gelfan, A. N., Harman, C., Kleidon, A., Bogaard, T. A., Wang, D., Wagener, T., Scherer, U., Zehe, E., Bierkens, M. F. P., Di Baldassarre, G., Parajka, J., van Beek, L. P. H., van Griensven, A., Westhoff, M. C., and Winsemius, H. C.: Advancing catchment hydrology to deal with predictions under change, Hydrol. Earth Syst. Sci., 18, 649–671, doi:10.5194/hess-18-649-2014, 2014.

Harman, C. and Troch, P. A.: What makes Darwinian hydrology "Darwinian"" Asking a different kind of question about landscapes, Hydrol. Earth Syst. Sci., 18, 417–433, doi:10.5194/hess-18-417-2014, 2014.

Hergarten, S., Winkler, G., and Birk, S.: Transferring the concept of minimum energy dissipation from river networks to subsurface flow patterns, Hydrol. Earth Syst. Sci., 18, 4277–4288, doi:10.5194/hess-18-4277-2014, 2014.

Kleidon, A.: Nonequilibrium thermodynamics and maximum entropy production in the Earth system, Naturwissenschaften, 96, 653–677, doi:10.1007/s00114-009-0509-x, 2009.

Kleidon, A. and Renner, M.: Thermodynamic limits of hydrologic cycling within the Earth system: concepts, estimates and implications, Hydrol. Earth Syst. Sci., 17, 2873–2892, doi:10.5194/hess-17-2873-2013, 2013.

Kleidon, A. and Schymanski, S.: Thermodynamics and optimality of the water budget on land: a review, Geophys. Res. Lett., 35, L20404, doi:10.1029/2008GL035393, 2008.

Kleidon, A., Zehe, E., Ehret, U., and Scherer, U.: Thermodynamics, maximum power, and the dynamics of preferential river flow structures at the continental scale, Hydrol. Earth Syst. Sci., 17, 225–251, doi:10.5194/hess-17-225-2013, 2013.

Kleidon, A., Renner, M., and Porada, P.: Estimates of the climatological land surface energy and water balance derived from maximum convective power, Hydrol. Earth Syst. Sci., 18, 2201–2218, doi:10.5194/hess-18-2201-2014, 2014.

Kollet, S. J.: Optimality and inference in hydrology from entropy production considerations: synthetic hillslope numerical

experiments, Hydrol. Earth Syst. Sci. Discuss., 12, 5123–5149, doi:10.5194/hessd-12-5123-2015, 2015.

McDonnell, J., Sivapalan, M., Vaché, K., Dunn, S., Grant, G., Haggerty, R., Hinz, C., Hooper, R., Kirchner, J., Roderick, M., Selker, J., and Weiler, M.: Moving beyond heterogeneity and process complexity: a new vision for watershed hydrology, Water Resour. Res., 43, W07301, doi:10.1029/2006WR005467, 2007.

Milly, P. C. D.: Climate, soil water storage, and the average annual water balance, Water Resour. Res., 30, 2143–2156, doi:10.1029/94WR00586, doi:10.1029/94WR00586, 1994.

Porada, P., Kleidon, A., and Schymanski, S. J.: Entropy production of soil hydrological processes and its maximisation, Earth Syst. Dynam., 2, 179–190, doi:10.5194/esd-2-179-2011, 2011.

Potter, N. J., Zhang, L., Milly, P. C. D., McMahon, T. A., and Jakeman, A. J.: Effects of rainfall seasonality and soil moisture capacity on mean annual water balance for Australian catchments, Water Resour. Res., 41, w06007, doi:10.1029/2004WR003697, 2005.

Rinaldo, A., Rodriguez-Iturbe, I., Rigon, R., Bras, R. L., Ijjasz-Vasquez, E., and Marani, A.: Minimum energy and fractal structures of drainage networks, Water Resour. Res., 28, 2183–2195, doi:10.1029/92WR00801, 1992.

Rodriguez-Iturbe, I., Rinaldo, A., Rigon, R., Bras, R. L., Ijjasz-Vasquez, E., and Marani, A.: Fractal structures as least energy patterns: The case of river networks, Geophys. Res. Lett., 19, 889–892, doi:10.1029/92GL00938, 1992.

Savenije, H. H. G.: The importance of interception and why we should delete the term evapotranspiration from our vocabulary, Hydrol. Process., 18, 1507–1511, doi:10.1002/hyp.5563, 2004.

Schaake, J., Cong, S., and Duan, Q.: The US MOPEX data set, IAHS-AISH P., 307, 9–28, 2006.

Schaefli, B., Harman, C. J., Sivapalan, M., and Schymanski, S. J.: HESS Opinions: Hydrologic predictions in a changing environment: behavioral modeling, Hydrol. Earth Syst. Sci., 15, 635–646, doi:10.5194/hess-15-635-2011, 2011.

Sivapalan, M., Blöschl, G., Zhang, L., and Vertessy, R.: Downward approach to hydrological prediction, Hydrol. Process., 17, 2101–2111, 2003.

Thompson, S., Harman, C., Troch, P., Brooks, P., and Sivapalan, M.: Spatial scale dependence of ecohydrologically mediated water balance partitioning: a synthesis framework for catchment ecohydrology, Water Resour. Res., 47, W00J03, doi:10.1029/2010WR009998, 2011.

van Genuchten, M. T.: A closed-form equation for predicting the hydraulic conductivity of unsaturated soils, Soil Sci. Soc. Am. J., 44, 892–898, doi:10.2136/sssaj1980.03615995004400050002x, 1980.

Wang, D. and Tang, Y.: A one-parameter Budyko model for water balance captures emergent behavior in darwinian hydrologic models, Geophys. Res. Lett., 41, 4569–4577, doi:10.1002/2014GL060509, 2014.

Wang, D., Zhao, J., Tang, Y., and Sivapalan, M.: A thermodynamic interpretation of Budyko and L'vovich formulations of annual water balance: proportionality hypothesis and maximum entropy production, Water Resour. Res., 51, 3007–3016, doi:10.1002/2014WR016857, 2015.

Wang, J. and Bras, R. L.: A model of evapotranspiration based on the theory of maximum entropy production, Water Resour. Res., 47, W03521, doi:10.1029/2010WR009392, 2011.

Westhoff, M. C. and Zehe, E.: Maximum entropy production: can it be used to constrain conceptual hydrological models?, Hydrol. Earth Syst. Sci., 17, 3141–3157, doi:10.5194/hess-17-3141-2013, 2013.

Westhoff, M. C., Zehe, E., and Schymanski, S. J.: Importance of temporal variability for hydrological predictions based on the maximum entropy production principle, Geophys. Res. Lett., 41, 67–73, doi:10.1002/2013GL058533, 2014.

Yang, H., Yang, D., Lei, Z., and Sun, F.: New analytical derivation of the mean annual water-energy balance equation, Water Resour. Res., 44, W03410, doi:10.1029/2007WR006135, 2008.

Zehe, E., Blume, T., and Blöschl, G.: The principle of "maximum energy dissipation": a novel thermodynamic perspective on rapid water flow in connected soil structures, Philos. T. R. Soc. B, 365, 1377–1386, doi:10.1098/rstb.2009.0308, 2010.

Zehe, E., Ehret, U., Blume, T., Kleidon, A., Scherer, U., and Westhoff, M.: A thermodynamic approach to link self-organization, preferential flow and rainfall–runoff behaviour, Hydrol. Earth Syst. Sci., 17, 4297–4322, doi:10.5194/hess-17-4297-2013, 2013.

Zehe, E., Ehret, U., Pfister, L., Blume, T., Schröder, B., Westhoff, M., Jackisch, C., Schymanski, S. J., Weiler, M., Schulz, K., Allroggen, N., Tronicke, J., van Schaik, L., Dietrich, P., Scherer, U., Eccard, J., Wulfmeyer, V., and Kleidon, A.: HESS Opinions: From response units to functional units: a thermodynamic reinterpretation of the HRU concept to link spatial organization and functioning of intermediate scale catchments, Hydrol. Earth Syst. Sci., 18, 4635–4655, doi:10.5194/hess-18-4635-2014, 2014.

Zhang, L., Hickel, K., Dawes, W. R., Chiew, F. H. S., Western, A. W., and Briggs, P. R.: A rational function approach for estimating mean annual evapotranspiration, Water Resour. Res., 40, w02502, doi:10.1029/2003WR002710, 2004.